Supplemental Data For:

INHIBITION OF EBOLA VIRUS ENTRY BY A C-PEPTIDE TARGETED TO ENDOSOMES

Emily Happy Miller[1,2], Joseph S. Harrison[1,3], Sheli R. Radoshitzky[4], Chelsea D. Higgins[3], Xiaoli Chi[4], Lian Dong[4], Jens H. Kuhn[5], Sina Bavari[4], Jonathan R. Lai[3], and Kartik Chandran[2]

[1]These two authors contributed equally to this work.

From the Departments of Microbiology and Immunology[2] and Biochemistry[3], Albert Einstein College of Medicine, Bronx, NY 10461; the United States Army Medical Research Institute of Infectious Diseases, Fort Detrick, Frederick, MD 21702[4]; and the Integrated Research Facility at Fort Detrick, National Institute of Allergy and Infectious Diseases, National Institutes of Health, Frederick, MD 21702 and Tunnell Consulting, Inc., King of Prussia, PA 19406[5]

Equilibrium Analytical Ultracentrifugation of Tat-Ebo and Lys-Ebo. Experiments were performed on a Beckman XL-1 with a Ti60 rotor. Purified peptides were dissolved in 20 mM phosphate (pH 7.6) containing 20 mM NaCl and loaded into 1.2 cm pathlength cells. Analysis was performed at several rotor speeds ranging from 20 to 45 krpm and at peptide concentrations ranging from 25 μM – 100 μM. At each rotor speed, samples were allowed to equilibrate for 24 hours and then high resolution radial spectra were recorded. For each sample, the data from several different rotor speeds and concentrations were fit globally to a single ideal species model using the program Heteroanalysis (Biotechnology/Bioservices Center, University of Connecticut, Storrs, CT). Non-linear regression was performed in accordance with the expression $c_r = c_o \exp [M(1-\nu\rho)\omega 2 (r^2-r_o^2)/2RT] + \text{base}$, where c_r is the concentration (in absorbance units) at radial position r, c_o is the concentration at an arbitrary reference position r_o near the meniscus, ν is the partial specific volume, ρ is the solvent density, ω is the rotor speed, R is the gas constant, T is the temperature, and base is a baseline absorbance correction to account for non-sedimenting species. Molecular weight estimates were obtained from the parameter *M*. Fits were judged to be adequate because there was no systematic deviation of residuals. Partial specific volumes of 0.7273 mL/g and 0.7452 mL/g were calculated for Tat-Ebo and Lys-Ebo based on amino acid composition, and a solvent density of 1.00182 g/mol was estimated using the program Sednterp (University of New Hampshire).

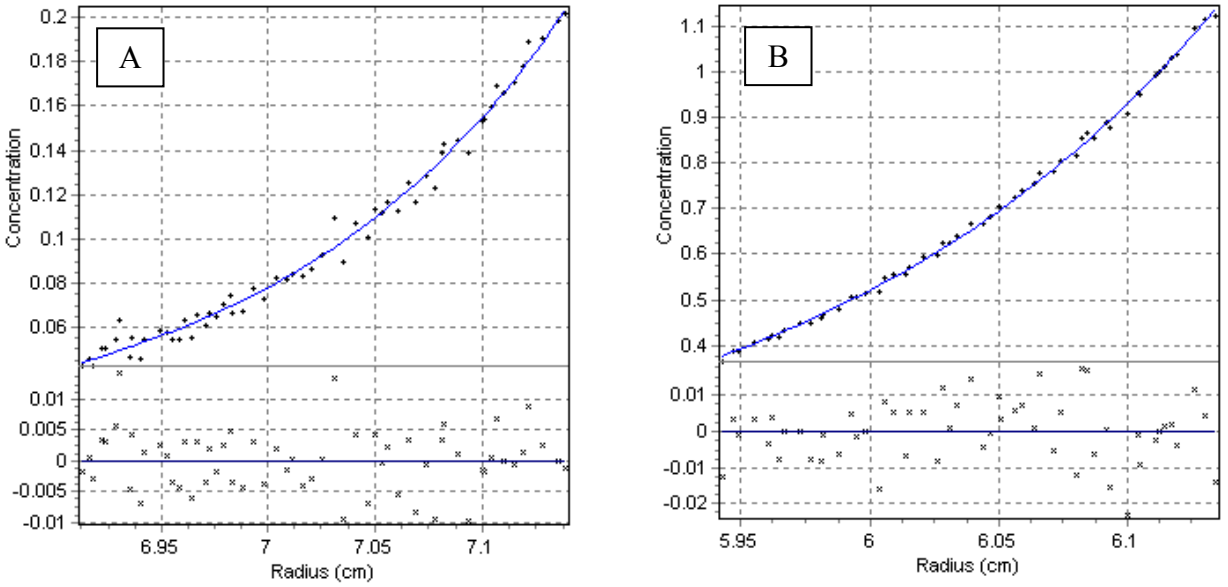

Figure S1. Representative analytical ultracentrifugation data for Tat-Ebo (A) and Lys-Ebo (B). Data were fit to a single ideal species model, resulting in molecular weight estimates of 4100 g/mol for Tat-Ebo (expected monomer molecular weight 4663 g/mol), and 4200 g/mol for Lys-Ebo (expected monomer molecular weight 3634 g/mol). Fits are shown as blue line and a plot of residuals shown below.

Cytotoxicity of Tat-Ebo. Cytotoxicity of Tat-Ebo peptide was assessed using the CytoTox-Glo assay kit (Promega). Vero cells were exposed to peptide (0-75 μM) for 2 h at 37 ^{o}C and then washed with PBS and fresh media was added. Luciferase activity (proportional to the activity of proteases released from dying or dead cells due to loss of plasma membrane integrity) was measured 14-16 h after peptide treatment. (Experiments performed in triplicate.) The peptide was well-tolerated over the range of concentrations used in the VSV-GP entry experiments (Figure S2).

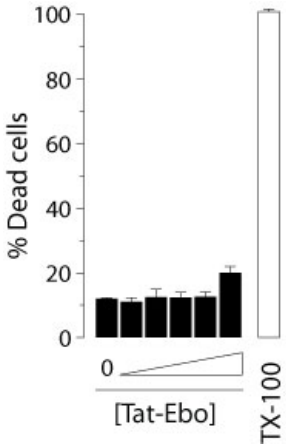

Figure S2. Cytotoxicity of Tat-Ebo.

Inhibition of entry by VSV-GP containing the mucin-like domain. Virus construction and entry inhibition experiments as described in the Materials and Methods. Results were comparable to inhibition of VSV-GP lacking the mucin domain.

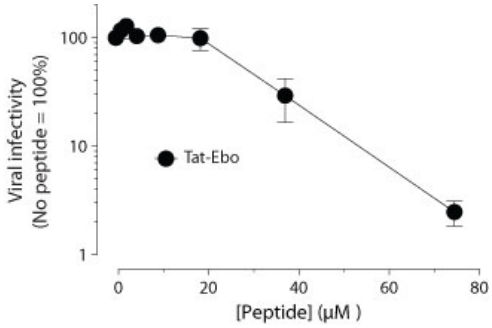

Figure S3. Inhibition of entry by VSV-GP containing the mucin-like domain.

Similarities in predicted contact residues among EboV and MarV CHR regions. We used the MarV GP2 ectodomain sequence to query the PDB and identify protein segments that are predicted to show structural homology. The two top hits were PDB ID 2EBO (one of the two EboV GP2 ectodomain structures in the putative 'post-fusion' conformation) and PDB ID 3CSY (the EboV GP1-GP2 'prefusion' structure). Since the 'post-fusion' conformation was most relevant to this study, we prepared a homology model in which the MarV sequence was threaded through the backbone coordinates for PDB ID 2EBO and then subjected this model to a round of energy minimization. We then compared the positioning and identity of residues on the C-peptide region that contact the NHR in the EboV structure with the MarV model (Figure S4). Several of the key contact residues in EboV (I619, I623, and I626) are identical in the MarV model. These three residues we found to be important for C-peptide activity in Tat-Ebo as well because these residues are altered in our Tat-Ebo^{3S} control. Other contact residues were not identical among EboV and MarV but were similar in terms of hydrophobicity. We believe these results explain the ability of the Tat-Ebo to inhibit marburg virus.

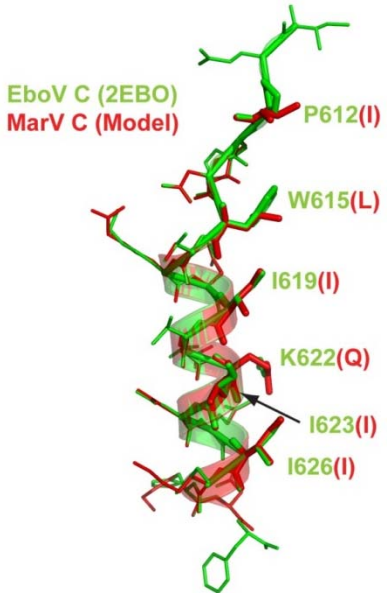

Figure S4. Overlay of C-peptide regions from the EboV crystal structure (PDB ID 2EBO, green) and the MarV model (red). The locations and identities of contact residues on the EboV are indicated in green and the identities of these residues in MarV shown in parentheses (red).